# FLOW CHARACTERISTICS IN AEROENGINE BEARING CHAMBERS WITH SHALLOW SUMP

**Budi Chandra**
Engineering Design and Mathematics,
University of the West of England,
Bristol, BS16 1QY, UK

**Kathy Simmons**
Gas Turbine and Transmissions Research Center,
University of Nottingham, University Park,
Nottingham, NG7 2RD, UK

## ABSTRACT

In an aeroengine oil is supplied to the bearings for lubrication and cooling. Subsequently, it creates a two phase flow environment in the bearing chamber that may contain droplets, mist, wall film, ligaments, froth or foam and liquid pools. After the oil has served its purpose, it is scavenged out of the chamber and recycled. Effective oil removal is essential as unnecessary working of the oil can lead to excessive heat generation in the chamber, increased risk of seal leakage, and reduced overall efficiency. However the task of oil removal is not trivial as it is entrained in a highly rotating environment induced by the rotating shafts.

Shallow sump variants were investigated using a design of experiments approach. A previous publication discussed the performance of the sump variants using categorization of visualization data relating to the extent of hydraulic uplift in the sump region. Hydraulic uplift was found to be directly related to residence volume in the gravity dominated wall film flow regime. Furthermore, it was found that the flow condition factors such as flow regime and shaft speed are the dominating factors affecting the hydraulic uplift severity. In terms of the geometrical factors, a deeper sump can reduce the hydraulic uplift severity. This reinforces the importance of sump depth, as a deeper sump tends to have lower residence volume but is often not implemented due to space constraint.

This paper presents further results from the experimental study on the shallow sump variants in terms of some important flow characteristics such as upstream flow detachment, upstream flow dry-out, and secondary flow. In addition to the geometrical factors, the flow condition factors such as the flow regime defined by how oil enters the chamber, flow rate, shaft speed, and scavenge ratio were investigated. Upstream flow detachment was observed only for cases where airborne droplets were present and at higher shaft speeds, also known as the windage dominated airborne droplets flow regime. It was noted that the geometrical factors are less important than the flow condition factors for upstream flow detachment as well as upstream flow dry-out and secondary flow.

## 1. INTRODUCTION

Scavenge oil flow in aeroengine bearing chamber continues to be a challenge for many aeroengine designers. Effective oil removal or scavenge is crucial to avoid unnecessary heat accumulation in the bearing chamber which can further degrade the oil properties and overall deterioration in heat transfer functionality. Oil removal from a bearing chamber is not trivial since fluid in the chamber is trapped in a highly rotating environment induced by fast rotating shafts. Figure 1 shows an illustration of the flow in a generic bearing chamber. Oil droplets are shed from the bearing and enter the chamber where windage induced by the rotating shaft dominates the flow field. Depending on the shaft speed, oil droplets can remain trapped in the highly rotating flow field. Subsequent oil droplets impact the chamber walls contributing to the wall film. The film is highly agitated due to the shearing air flow resulting in a significant amount of oil being stripped from the film and rejoining the bulk rotating flow. A bearing chamber employs a sump to facilitate oil scavenge. It provides a pocketed region to collect the oil where the oil is then scavenged out through an off-take pipe by a scavenge pump.

A scavenge pump helps to remove oil from the bearing chamber, however its effectiveness is often hindered by gas ingestion into the off-take pipe including the unavoidable dispersed gas phase in the oil itself. The gas in the chamber has lower density than the oil, and therefore simply increasing the pump capacity will increase the proportion of the ingested gas phase compared to the liquid phase. An excessive amount of ingested gas will eventually reduce the flow area for the oil to drain through resulting in an increase in both the oil residence time and residence volume in the chamber. However, if designed correctly, the sump geometry itself can improve the oil scavenge performance to some degree.

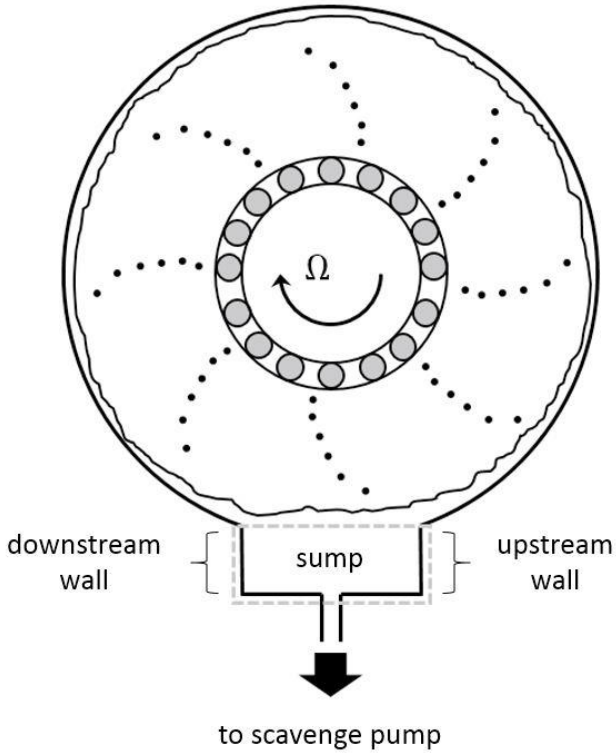


**FIGURE 1: OIL SHEDDING, WALL FILM AND SUMP FLOW IN A GENERIC BEARING CHAMBER.**

Knowledge of what constitutes a good sump geometry as well as the ability to assess its performance across a range of operating conditions is imperative. The majority of initial work on bearing chamber flow was carried out by the Institut für Thermische Strömungsmaschinen at Karlsruhe Institut für Technologie, Germany. Early investigations included film thickness measurement in a simplified generic bearing chamber using an ultrasonic approach [1]. The work was extended to film thickness measurement using capacitive probes and film velocity measurement using laser Doppler velocimetry [2, 3]. Furthermore, the droplets' flow and size distribution were also investigated [4, 5 and 6]. A study on a particular sump design with a lid akin to the one employed in the Rolls-Royce BR725 engine was performed as well [7]. The study focused on the impact of various design parameters on the overall scavenge capture efficiency. A more recent study extended to an investigation into seal leakage [8, 9].

A systematic research program on bearing chamber scavenge flow comprising of experimental and computational elements was conducted at the Gas Turbine and Transmissions Research Center at Nottingham University, UK (previously Rolls-Royce University Technology Centre in Gas Turbine Transmission Systems). The experimental aspect of the research programme aimed to achieve several objectives:

- Performance assessments of engine representative sump geometries at representative shaft speeds and liquid flow rates.
- Application and development of required experimental techniques.
- Generation of validation data for analytical work and CFD modelling.
- Development of an optimised scavenge geometry for future engines.
- Generation of design rules for shallow sumps.

The research program started with investigations into generic deep sumps with dimensions typical of Internal Gear Box (IGB) sumps of Rolls-Royce Trent family engines [10, 11]. Representative shallow engine sumps were investigated and their performances compared [12]. It was found that a derivative of the Rolls-Royce AE3007 centre sump dubbed Curved Wall Deep Sump (CWDS) has superior performance compared to some of the other sump designs. A 3D CAD model of CWDS and its manufactured form in acrylic are shown in Figure 2.

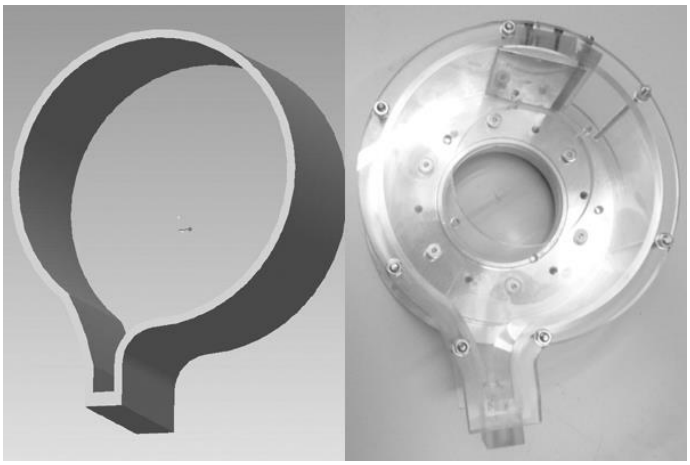

**FIGURE 2: CURVED WALL DEEP SUMP (CWDS) - SHAFT ROTATIONAL DIRECTION IS CLOCK-WISE.**

The CWDS can maintain low residence volume in various flow conditions and a fairly calm flow with minimum liquid pooling in the sump and a low level of liquid re-entrainment. This reinforced the importance of previous findings on some design features, particularly the sump depth [13, 14 and 15]. Furthermore, it was proposed that the superior performance of CWDS is attributed to some of its design features described in the following paragraphs:

*Upstream wall curvature*

This feature helps to gradually decrease the incoming liquid momentum and directs the flow towards the sump's off-take. It also helps to keep the liquid attached to the wall, reducing the risk of overshoot. However care should be taken to ensure that the curvature matches with the flow conditions. If the radius of curvature is too small for a given incoming liquid momentum, the flow can overshoot and bypass the sump. On the other hand, if the radius of curvature is too big, the flow into the off-take hole has to turn more to compensate for the shallower approach angle. Given that the momentum of the incoming liquid is generally high, there is a risk of developing a more severe hydraulic uplift due to the required flow turning, which in turn contributes to an increase in residence volume. In this context, hydraulic uplift is characterized by excessive pooling or bulging of liquid in or near the sump due to sudden reduction in the momentum of the incoming flow, i.e. Froude number is abruptly changed from supercritical to subcritical.

*Downstream wall curvature*

The purpose of the downstream wall is to contain the liquid in the sump. If the incoming liquid momentum is relatively high (for example at high shaft speed), a near vertical downstream wall can encourage an abrupt flow transition from supercritical to subcritical. This can result in a more severe hydraulic uplift thus increasing the likelihood for higher residence volume. On the other hand, if the downstream wall angle is too shallow, liquid in the sump cannot be contained and can continue to travel uphill. The shape of the CWDS downstream wall was designed to avoid abrupt flow transition (from supercritical to subcritical) but is still capable of reducing downstream liquid carry-over.

*Sump depth*

A deep pocket or slot such as found in the CWDS helps to shelter the gathered liquid away from the highly rotating environment in the chamber. It minimizes the chance for the liquid in the sump to be entrained back into the bulk rotating flow. Therefore a deeper sump is preferable. However, other engine requirements limit the amount of available space to accommodate the extra depth.

The purpose of this study is to investigate the effect of each of these design features of CWDS. Given that in many situations a deep sump cannot be employed, a shallower version of CWDS, dubbed Curved Wall Shallow Sump (CWSS), was investigated. The tests were conducted at various engine representative flow conditions (inlet flow rates, scavenge ratios, shaft speeds). Visual observations were carried out to identify various flow features in the chamber, especially in the vicinity of the sump region. All visualizations were done with "naked eye" without aid of dye or laser light sheet. Design of Experiments (DOE) is employed to facilitate selection of test configurations and analysis of the results.

In a previous study, a rigorous parametric study on CWSS was conducted. The experimental work considered various design parameters (upstream and downstream sump wall curvatures, sump width, depth, and orientation) tested at various flow conditions (inlet system, inlet flow rate, scavenge ratio, shaft speed). Results of this parametric study on the effect of geometrical and flow condition factors on the hydraulic lift severity of liquid in the sump have been published [16]. It was found that the flow condition factors (inlet

system and shaft speed) are the most dominating factors for the severity of hydraulic uplift. Of all the geometrical factors tested, the sump depth is the most important factor where a deeper sump can reduce the severity of hydraulic uplift.

This paper presents further results of the parametric study focusing on other measures of scavenge performance, i.e. the effect of the geometrical and flow condition factors on upstream flow detachment, upstream flow dry-out, and secondary flow. Upstream flow detachment is undesirable since it can potentially increase the risk of unnecessary liquid recirculation in the chamber, thus increasing the residence time and volume. Upstream flow dry-out is also undesirable since it can lead to a non-uniform heat transfer on the chambers walls and possibly oil coking. The presence of a secondary flow in a bearing chamber as described in [13] and [14] can increase the risk for seal leakage, and therefore it needs to be avoided as well.

## 2. NOMENCLATURE AND ABBREVIATIONS

| | |
|---|---|
| dR | Sump depth |
| $Q_G$ | Gas flow rate |
| $Q_L$ | Liquid flow rate |
| $Q_T$ | Total two-phase exit flow rate |
| R1 | Chamber radius |
| R2 | Downstream sump wall radius |
| R3 | Upstream sump wall radius |
| SR | Scavenge ratio |
| w | Sump width |
| $\theta$ | Sump orientation |
| $\Omega$ | Shaft speed |

| | |
|---|---|
| DOE | Design Of Experiment |
| CWDS | Curved Wall Deep Sump |
| CWSS | Curved Wall Shallow Sump |
| FG | Film Generator |
| IS | Inlet System |
| RID | Rotating Inlet Distributor |

## 3. TEST FACILITY

An experimental test rig (see Figure 3) was built for investigating scavenge flow in a bearing chamber. A significant asset of the test rig is its versatility to accommodate various chamber and sump geometries. All chambers that were utilized in this test campaign were manufactured out of transparent acrylic to allow for unobstructed flow observations. The main rotor is a stub shaft fitted with a hollow cylinder to simulate an engine shaft. The hollow cylinder also functions as a Rotating Inlet Distributor (RID) described later. The drive shaft extends to the rear of the chamber and is supported by two grease packed ball bearings. Two accelerometers and two thermocouples are used to monitor the vibration level and temperature of the bearings. A belt connects the drive shaft to a 22 kW DC motor.

Water was chosen as the working fluid due to its ease of handling and associated rig costs. Some of the relevant properties of water at room temperature are similar to those of Mobil Jet Oil II at typical aero-engine bearing chamber operating temperatures. Water density at 20°C is about 1000 kg/m$^3$ and oil density at 150°C is about 970 kg/m$^3$. The viscosity of water at 20°C and oil at 150°C are similar (0.001 Ns/m$^2$). However, surface tensions are quite different. Water at 20°C has surface tension of about 0.07 N/m, and oil at 150°C has surface tension of about 0.03 N/m. Film flow observed in the bearing chamber is highly disturbed and mainly driven by the windage especially at high shaft speeds. In this condition, surface tension may not play a significant role. It is realized that flow features being investigated such as flow detachment and dry-out can be influenced by surface tension. Therefore the exact onset of those flow features may not be the same if oil is used, however evidences of a trend between a factor and a particular flow feature found in this study are still quite useful.

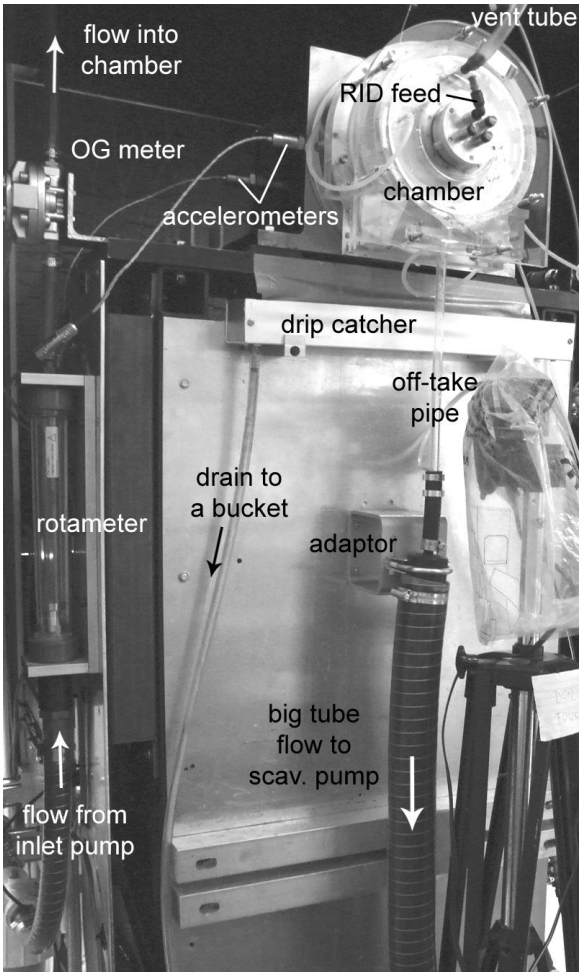


**FIGURE 3: SCAVENGE FLOW TEST RIG.**

The rig is open to atmosphere, hence all tests were carried out at ambient pressure. There is no dedicated vent line. All liquid and any ingested gas are taken out through a single scavenge port. A breather hole on the front plate of the chamber is fitted with a vent tube and opens to atmosphere to allow inflow (and outflow) of air.

The rig employs a circuit of pipe work which carries water and air (Figure 4). In this circuit, water flows in a closed loop, whereas air flows in an open loop. A sealed polyethylene baffled water tank is used as a reservoir and also functions as a liquid/gas separator to allow for gas flow rate measurement.

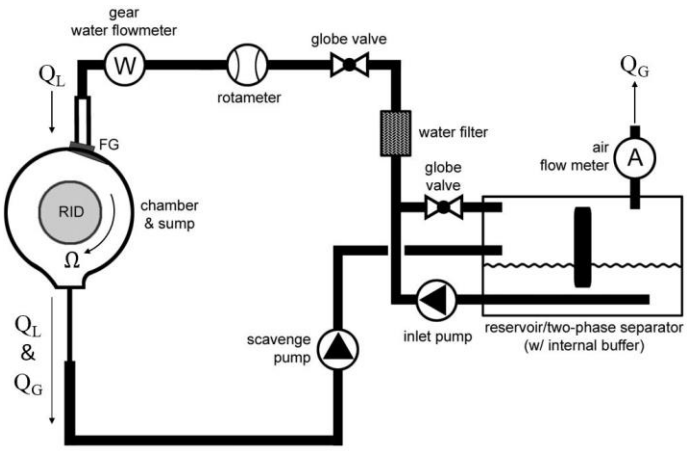


**FIGURE 4: FLOW CIRCUIT.**

Water from the reservoir is drawn by a centrifugal inlet pump and is directed into the chamber via two types of inlet systems: FG (Film Generator) and RID (Rotating Inlet Distributor). Each inlet system was utilized independently. FG, as the name suggests, introduces water into the chamber as wall film only. Whereas RID introduces water into the chamber as droplets shedding off the shaft (hollow cylinder). These two types of inlet systems represents two extrems. In a typical aero-engine bearing chamber, oil can be present in both droplet form and wall film. For more detailed descriptions of each inlet system, please refer to the previous publications [12, 17].

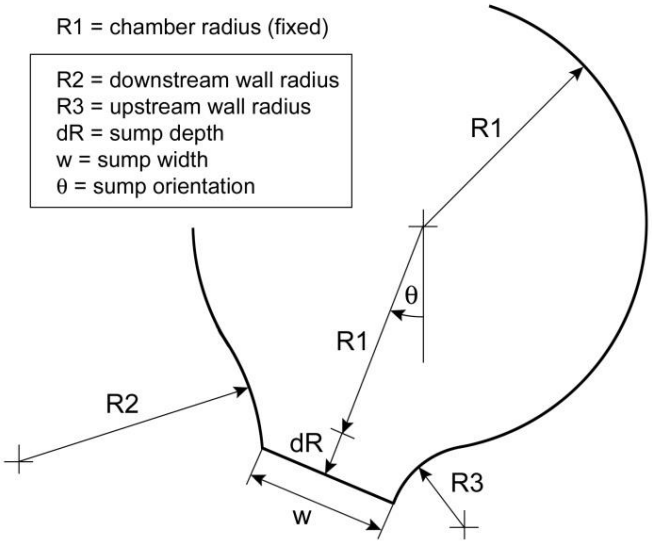


**FIGURE 5: GEOMETRIC PARAMETERS OF CWSS (R1 IS FIXED).**

Previous work has shown that a CWDS derivative of the Rolls-Royce AE3007 centre sump performs relatively well compared to some other designs. The defining features of a CWDS are its upstream and downstream radii, width and depth, as well as its relative orientation in the chamber. These five factors were chosen as the parameters to be studied for CWSS with a strict constraint for a much shallower sump compared to CWDS. In a CWDS, the sump depth can be more than 20% of the chamber's radius. Figure 5 illustrates those geometric parameters. Note that in this parametric study, the chamber radius, R1 is a fixed value. The diameter of the scavenge off-take pipe is fixed at 0.1 R1 and is located centrally on the sump base.

A parametric study was conducted using a Design of Experiments (DOE) approach. Two values representing a low and a high of each geometric parameter are assigned. A full factorial design with five factors would require 32 unique sumps. To obtain the main effects and second-order interactions, it is sufficient to analyse a half fraction factorial resolution V design requiring only 16 unique sumps. In resolution V designs, no-main-effect or two-factor interaction is confounded with any other main effect or two-factor interaction [18]. MINITAB™ was used to construct the half factorial design and to analyse the test results.

Table 1 lists the low and high values of each geometric parameter. The vertical off-take of CWDS (Figure 2) is not located at bottom dead centre. In this parametric study, the off-take was either located vertically at bottom dead centre ($\theta = 0°$) or angled at 15° along a radial line. The angled orientation is more similar to the CWDS than the vertical orientation, but neither is exactly the same.

**TABLE 1: EXTREMA OF GEOMETRIC PARAMETERS.**

| Parameter | Low Value | High Value |
|---|---|---|
| dR | 0.04 $R_1$ | 0.15 $R_1$ |
| $R_2$ | dR | $R_1$ |
| $R_3$ | dR | $R_1$ |
| w | 0.1 $R_1$ | 0.3 $R_1$ |
| $\theta$ | 0° | 15° |

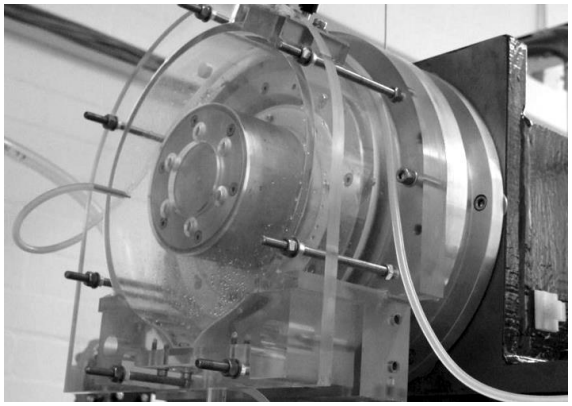

**FIGURE 6: CONFIGURATION ZERO.**

In addition to the 16 unique sump configurations, a centre point (configuration zero) was also tested with a mean value for each of its geometric parameters, except the orientation, θ which was chosen to be 0°. Figure 6 shows a close-up of configuration zero installed on the test rig. Configuration zero is not a true centre point since θ is not the mean value. In the analysis, this centre point is not considered. Nevertheless, conclusions can still be drawn based on linear responses of the model.

Acrylic block attachments were manufactured to form each sump configuration. Each configuration is formed by two block attachments. Figure 7 illustrates the assembly of the chamber including the sump region for a given sump configuration. The base of the sump is formed by a flat acrylic plate. Extra care in manufacturing and assembly was taken to ensure that the block attachments are fully flush with the main housing where the transition is nominally smaller than typical film thickness (50-100 microns).

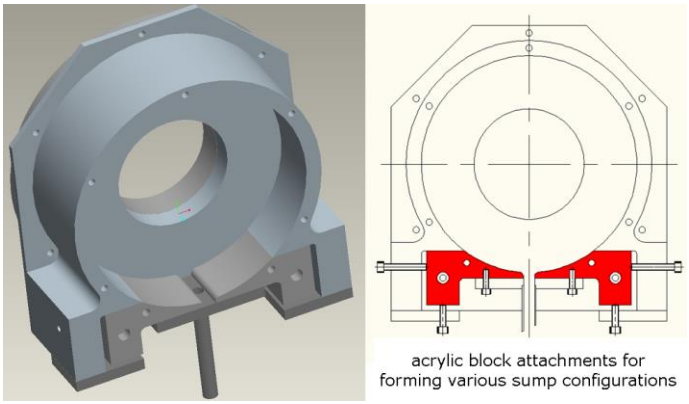


**FIGURE 7: CHAMBER ASSEMBLY FOR A GIVEN SUMP CONFIGURATION.**

For the flow condition factors, three inlet flow rates ($Q_L$ = 2.69, 3.37 and 4 litres per minute) were investigated for each sump configuration using either FG or RID. For each inlet flow rate, four scavenge ratios were tested (SR = 1.2, 1.5, 2 and 4). And for each combination of flow rate and scavenge ratio, 4 shaft speeds were tested (Ω = 0 for FG or 1000 rpm for RID, 5000, 10000 and 15000 rpm). The scavenge ratio, SR is defined as the ratio of total exit volume flow rate, $Q_T$ to inlet liquid volume flow rate, $Q_L$ where $Q_T$ is the sum of $Q_L$ and gas flow rate in the off-take, $Q_G$. The gas flow rate is measured for gas flow leaving the reservoir (see Figure 4) using a diaphragm gas flowmeter for average values and thermal mass flowmeter for instantaneous values. The scavenge ratio can be varied by changing the scavenge pump speed.

## 4. RESULTS

MINITAB™ assigns a coded level for each of the extrema. A level 0 is coded for the low value, and a level 1 for the high value or the designated inlet system (IS). Additional levels were used to code the values for liquid flow rate, scavenge ratio and shaft speed. Table 2 lists the assigned coded levels for each flow condition and geometrical factor, and their corresponding actual values.

**TABLE 2: CODED LEVELS AND CORRESPONDING VALUES.**

| Factor | Coded Levels | Values |
|---|---|---|
| dR | -1, +1 | 0.04 R1, 0.15 R1 |
| R2 | -1, +1 | dR, R1 |

| | | |
|---|---|---|
| R3 | -1, +1 | dR, R1 |
| w | -1, +1 | 0.1 R1, 0.3 R1 |
| θ | -1, +1 | 0°, 15° |
| IS | -1, +1 | FG, RID |
| $Q_L$ | -1, 0, +1 | 2.69, 3.37, 4 lpm |
| SR | -3, -1, +1, +3 | 1.2, 1.5, 2, 4 |
| Ω | -3, -1, +1, +3 | 0(FG)/1k(RID), 5k, 10k, 15k rpm |

### 4.1 Upstream Flow Detachment

The *upstream flow* is defined as the flow of liquid, primarily in the wall film, just prior to entering the sump. Ideally, the upstream flow stays attached to the chamber wall until it reaches the sump. However, due to high windage-induced shear and certain geometrical factors, the upstream flow can detach prematurely prior to entering the sump. This flow detachment is undesirable since it can potentially increase the risk of unnecessary liquid recirculation in the chamber, thus increasing the residence time and volume.

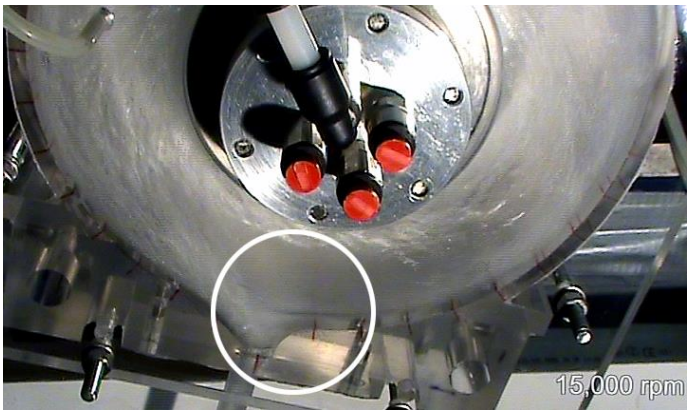


**FIGURE 8: UPSTREAM FLOW DETACHMENT WAS OBSERVED.**

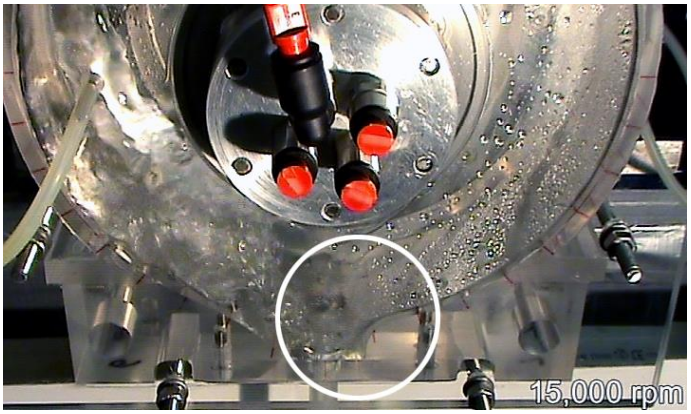


**FIGURE 9: UPSTREAM FLOW DETACHMENT WAS NOT OBSERVED.**

Visual observation based on video footage was conducted across all configurations in various flow conditions to survey whether an upstream flow detachment occurs or does not occur. DOE analysis was conducted to see the effect of various geometrical and flow condition factors. The coded values for each factor are as listed in Table 2. The response in this case has only two levels (0 for not detached, and 1 for detached including partial detachment). Typical flows with and without detachment are shown in Figure 8 and Figure 9 respectively.

The matrix plot of the flow condition and geometrical factors on the flow detachment is shown in Figure 10. It shows that flow detachment exists exclusively for cases with RID and at the higher shaft speeds (Ω = 10000 and 15000 rpm). In all FG cases, no upstream flow detachment can be found. Therefore flow detachments can be attributed to the higher liquid momentum induced by the impacting droplets.

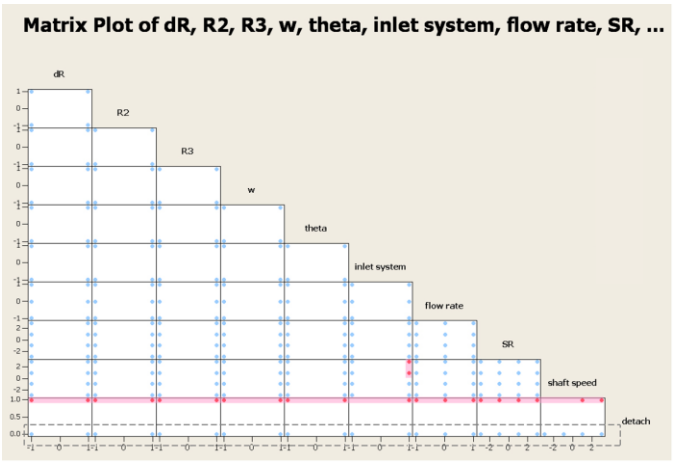


**FIGURE 10: MATRIX PLOT OF FACTORS AFFECTING UPSTREAM FLOW DETACHMENT.**

The interaction plot and the main effects plot for upstream flow detachment are shown in Figure 11 and Figure 12 respectively. It also emphasizes the same conclusions drawn from the matrix plot. Flow detachments exist only when the inlet system is RID and the shaft speed is 10000 or 15000 rpm.

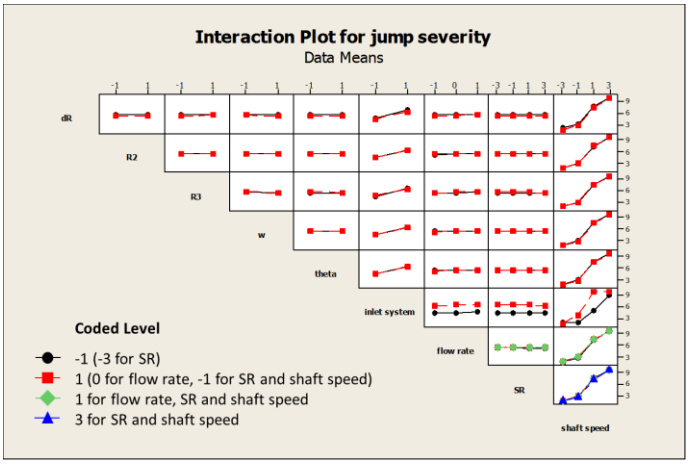


**FIGURE 11: INTERACTION PLOT FOR UPSTREAM FLOW DETACHMENT.**

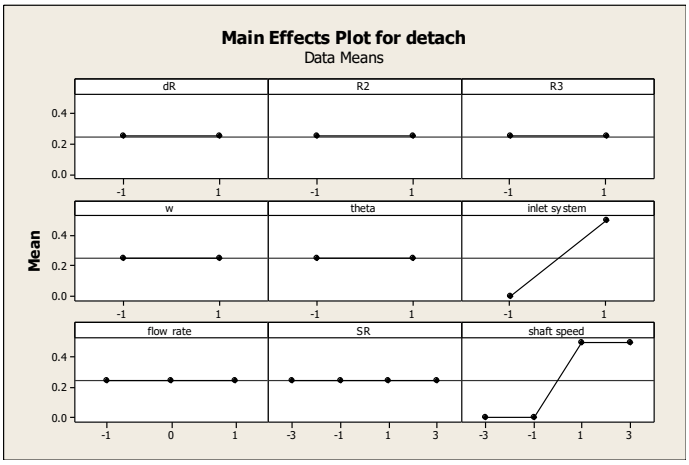


**FIGURE 12: MAIN EFFECTS PLOT FOR UPSTREAM FLOW DETACHMENT.**

In terms of avoiding upstream flow detachment, it is desirable to introduce the liquid into the chamber with less initial momentum and keep it as low as possible. This can be achieved via the use of FG, i.e. introducing the liquid as wall film only or via the use of structures to disrupt the momentum of the shedding droplets from the RID. In cases where shedding droplets cannot be avoided, operating the shaft at lower speeds may help to reduce the risk of upstream flow detachment. However this is often in conflict with other engine requirements.

### 4.2 Upstream Flow Dry-out

Liquid film dry-out can occur due to a thinning of the film by a high shearing air flow induced by the shaft rotation. The thinning of the film can be due to the geometrical factors which leave the film more exposed to the shearing air flow in the chamber. The film condition can also be dictated by the flow condition factors such as the liquid flow rate and shaft speed themselves. An upstream flow dry-out on the chamber wall is undesirable since it can lead to non-uniform heat transfer and possibly oil coking. Sample screen captures showing comparison of flow with and without upstream flow dry-out are given in Figure 13 and Figure 14.

Unsurprisingly, flow dry-out on the upstream wall can only occur when the liquid flow in the chamber is introduced as film (FG). If the liquid in the chamber is introduced as droplets (RID), upstream flow dry-out can never occur unless there exists a structure between the shaft and the chamber wall, such as a bearing support mount.

DOE analysis was conducted to see the effect of the various factors on the occurrence of dry-out. The values of flow condition and geometrical factors were coded according to Table 2. The response in this case is only two levels: 0 for no dry-out and 1 for when dry-out occurs. The residual plots for upstream flow dry-out are shown in Figure 15. The normal probability plot shows that the results mostly lie along a normal distribution line.

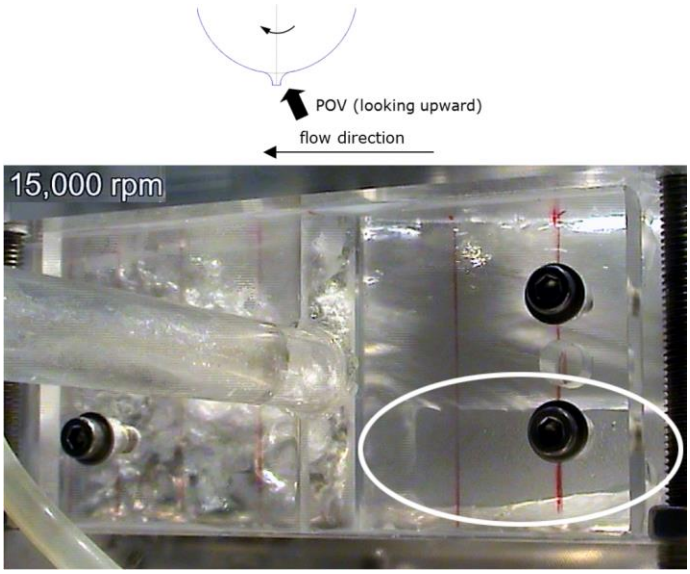


**FIGURE 13: UPSTREAM FLOW DRY-OUT WAS OBSERVED.**

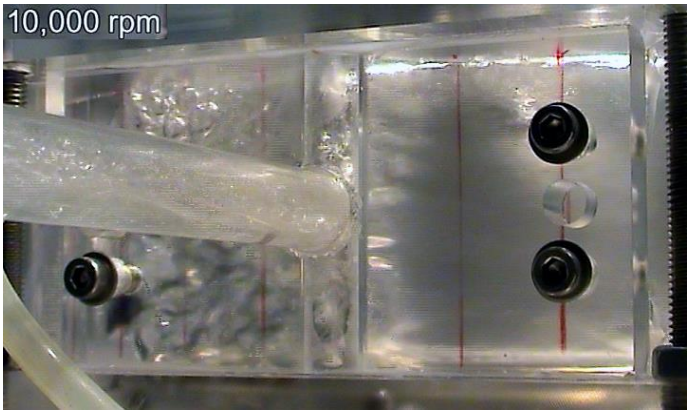


**FIGURE 14: UPSTREAM FLOW DRY-OUT WAS NOT OBSERVED.**

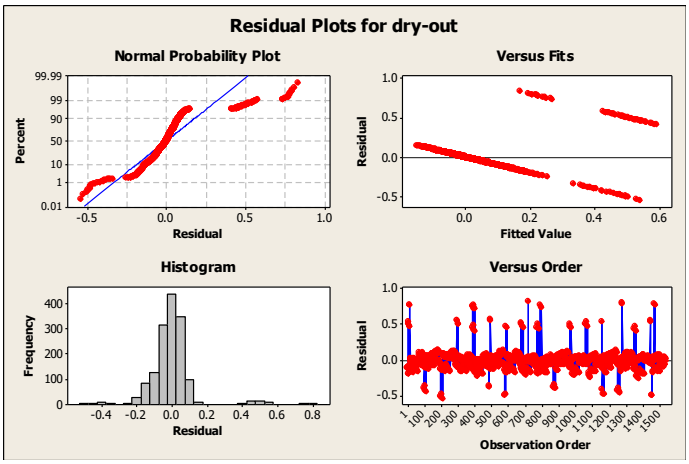


**FIGURE 15: RESIDUAL PLOTS FOR UPSTREAM FLOW DRY-OUT.**

The interaction plot is shown in Figure 16. It emphasizes the fact that there is no dry-out for all RID cases. In FG cases, the lowest liquid flow rate poses greatest risk of dry-out. Also in FG cases, the risk of dry-out increases as the shaft speed increases from 10000 rpm to 15000 rpm. Also notice that a wider sump reduces the risk of dry-out if the upstream radius is low (curvier), but increases the risk if the upstream radius is high (flatter). There are few other interactions but the effects are almost negligible.

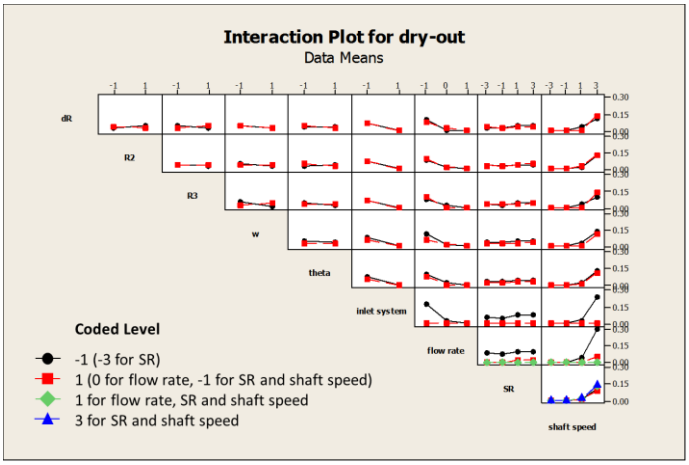


**FIGURE 16: INTERACTION PLOT FOR UPSTREAM FLOW DRY-OUT.**

The main effects plot is shown in Figure 17. The upstream flow dry-out is mostly influenced by shaft speed, liquid flow rate, and inlet system. The scavenge ratio and the geometrical factors have insignificant effects. In terms of the geometrical factors, the order of significance and the corresponding desired values for each factor are:

1. Sump width, w = +1 (wider)
2. Orientation, θ = +1 (rotated)
3. Upstream wall radius, R3 = -1 (curvier)
4. Downstream wall radius, R2 = -1 (curvier)
5. Sump depth, dR = +1 (deeper)

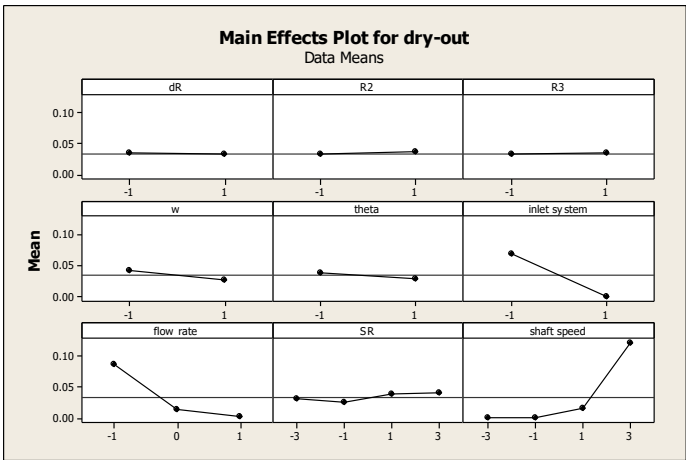


**FIGURE 17: MAIN EFFECTS PLOT FOR UPSTREAM FLOW DRY-OUT.**

Those favorable values of geometrical factors correspond to a configuration that was also identified as one of the best configurations for the least hydraulic uplift [16]. This may suggest that upstream wall film coverage and jump severity level are related. A lower jump severity level means liquid stays in the sump region as a mostly stagnant pool and therefore it helps to wet the surrounding walls. Vice versa, if the jump severity level is high, more liquid is carried downstream thus less is available in the sump region and therefore dry-out on the upstream wall is more likely to occur.

The effects of geometrical factors are quite small compared to some flow condition factors. In order to avoid dry-out, it is recommended to have low shaft speed, high flow rate, and IS = RID. In fact by using RID alone, it is enough to avoid dry-out. However in the engine, the shedding droplets are often obstructed by various structures so that a complete coverage of chamber wall by the virtue of droplets shedding alone is not feasible. Increasing the liquid flow rate can also reduce the risk of upstream flow dry-out, however it may conflict with other requirements such as to keep the residence volume at a minimum and a slower shaft speed may conflict with other engine requirements.

## 4.3 Secondary Flow

There exists a boundary layer flow on the stationary end-walls (front and rear face plates) of a bearing chamber. Outside this boundary layer, pressure balances centrifugal force. Inside the boundary layer, the flow is viscous and its velocity magnitude is much less. In the boundary layer, there is no pressure gradient normal to the wall. A liquid droplet sitting on the end-wall will only experience a pressure gradient in the radial direction. Since the pressure away from the shaft is greater than the pressure near the shaft, the droplet will be pushed toward the shaft while staying in contact with the wall. This flow in the boundary layer that pushes liquid radially inward and toward the shaft is termed secondary flow. The secondary flow combined with the windage drives the droplet to follow an inward spiraling path towards the shaft.

Depending on the geometrical factors and the flow conditions in the chamber, there can be varying degrees of liquid pooling in the sump region. This liquid will interact with the secondary flow causing some droplets to travel up to the shaft along the vertical wall of the chamber. This secondary flow can potentially cause leakage if the bearing is not properly sealed and also may lead to a higher oil residence time.

**TABLE 3: SECONDARY FLOW CATEGORIES.**

| Secondary Flow Category | Descriptions |
|---|---|
| 0 | No secondary flow |
| 1 | Broken, thin, incomplete bridging |
| 2 | Broken, thick, intermittent bridging |
| 3 | Continuous, thin |
| 4 | Continuous, thick |

DOE analysis was conducted on various geometrical and flow condition factors and their effects on the occurrence and severity of secondary flow. The coded levels and the corresponding actual values of the factors are listed in Table 2. The responses are categorized according to the degree of severity of the secondary flow and are listed in Table 3. These categories of secondary flows are based on previous observations spanning various chamber and sump geometries such as a tangential sump [13, 14 and 15], generic IGB deep sump [10, 11] and CWDS [12].

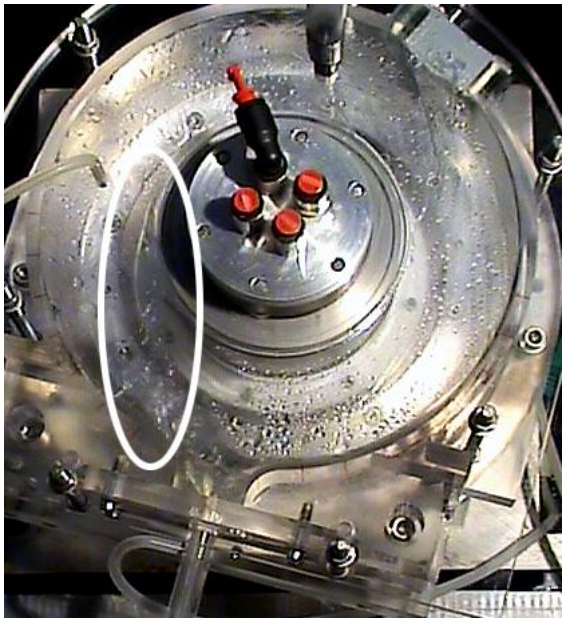

**FIGURE 18: SECONDARY FLOW CATEGORY 1 (BROKEN, THIN, INCOMPLETE BRIDGING).**

Figure 18 and Figure 19 show screen captures of some typical secondary flows. In this parametric study, only secondary flows of up to category 2 were observed. All secondary flows are of the broken types; there are no secondary flows that are continuous stemming from the root (liquid pooling) to the shaft. Therefore the response observed in this study has only 3 categories: category 0, 1, and 2.

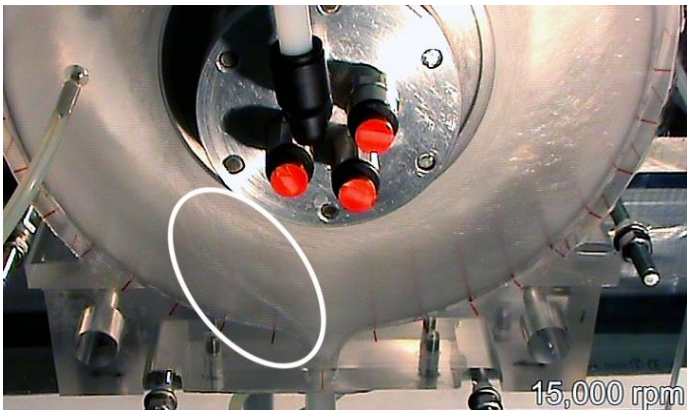


**FIGURE 19: SECONDARY FLOW CATEGORY 2 (BROKEN, THICK, INTERMITTENT BRIDGING).**

Figure 20 shows the residual plots for secondary flow. Notice that some responses deviate from a normal distribution (highlighted by the boxes in the figure). The histogram shows that these anomalies are only representing a small number of samples, but the occurrences of the secondary flows were confirmed in the video observations.

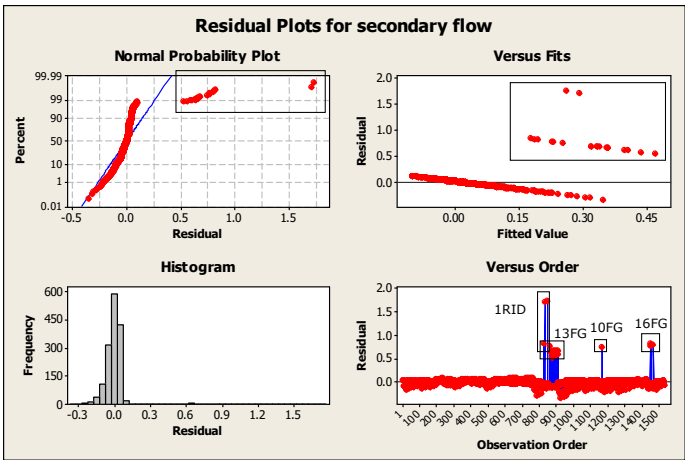


**FIGURE 20: RESIDUAL PLOTS FOR SECONDARY FLOW.**

The interaction plot for secondary flow is shown in Figure 21. Notice that secondary flows happen only at the highest shaft speed ($\Omega = 15000$ rpm). However if the sump depth is shallow, secondary flow never happens, even at $\Omega = 15000$ rpm. In fact, a shallow sump is a sufficient condition to make sure that secondary flow never occurs. There are few other interactions but they have only small or almost negligible effects. For example, changing the inlet system from FG to RID helps to reduce the risk of a secondary flow when the sump is rotated ($\theta = 15°$), but makes it slightly worse if the sump is vertical ($\theta = 0°$).

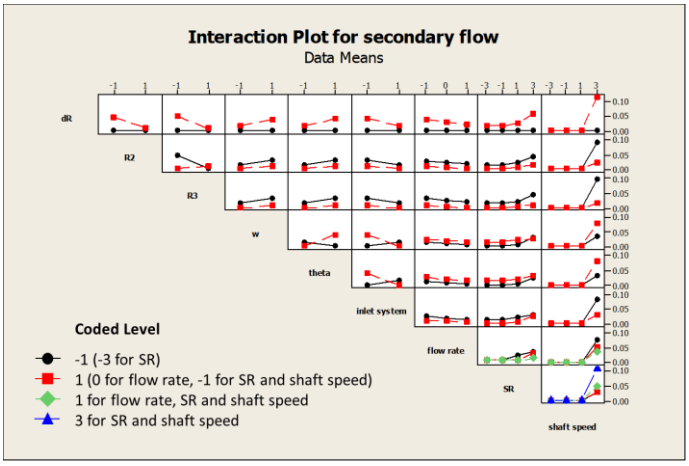


**FIGURE 21: INTERACTION PLOT FOR SECONDARY FLOW.**

The main effects plot for secondary flow is shown in Figure 22. The most significant factor is the shaft speed. In fact, secondary flow can be avoided solely by keeping the shaft speed at or below 10000 rpm.

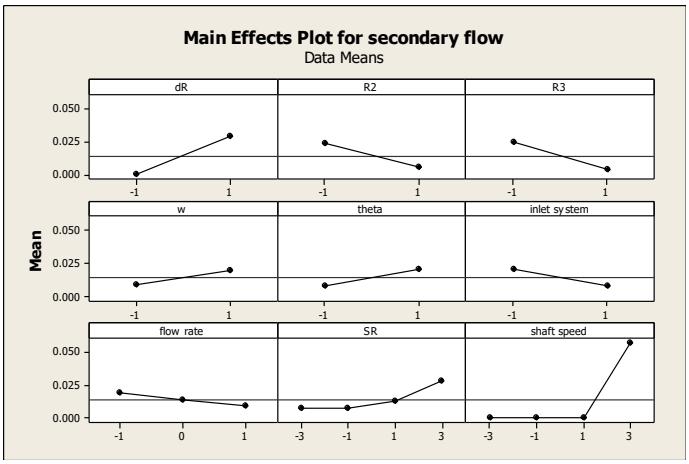


**FIGURE 22: MAIN EFFECTS PLOT FOR SECONDARY FLOW.**

In order to avoid or keep the secondary flow at minimum level, the following is the list of flow condition factors and their corresponding recommended values, from the most to the least significant:

1. Low shaft speeds ($\Omega \leq 10000$ rpm)
2. SR $\leq 1.5$
3. IS = RID
4. High flow rate ($Q_L$ = 4 lpm)

As shown by the interaction plot (Figure 21), a shallow sump is enough to ensure that no secondary flow occurs. If the sump happens to be deep, the other geometrical factors can be tweaked to minimize the secondary flow. Considering only the geometrical factors, the following is a list of their recommended values from the most significant factor to the least:

1. Sump depth, dR = -1 (shallower)
2. Upstream wall radius, R3 = +1 (flatter)
3. Downstream wall radius, R2 = +1 (flatter)
4. Sump width, w = -1 (narrower)
5. Orientation, $\theta$ = -1 (vertical)

The results suggest that a shallower sump is good to suppress or minimize secondary flow. A secondary flow usually stems from a relatively stagnant liquid pooling combined with a strong pressure gradient between the shaft and chamber wall induced by the shaft rotation. In a shallow sump, when the windage is strong (high shaft speed) liquid pooling is highly disturbed and most liquid is stripped and carried away upstream. There is no stagnant liquid pooling, and therefore secondary flow cannot properly develop.

It has been shown that for minimizing hydraulic uplift severity [16] and upstream flow dry-out occurrence, a deeper sump is favorable. There is clearly a conflict of interest between minimizing hydraulic uplift severity or upstream flow dry-out and suppressing a secondary flow. However it is perhaps wise to prioritize for minimizing hydraulic uplift and dry-out, since in an aero-engine a secondary flow is less likely to develop. Various structures in the bearing chamber may disrupt the radial pressure gradient from the chamber wall to the shaft, thus preventing a fully developed secondary flow. If a secondary flow still persists, a secondary flow management device in the form of an annular fence ring attached to the end-wall of a bearing chamber can be used. Fences have been tested successfully to reduce or eliminate secondary flow in a bearing chamber [13, 15].

## 5. CONCLUSIONS

Table 4 summarizes preferred values of flow condition and geometrical factors for investigated flow characteristics (upstream flow detachment, upstream flow dry-out and secondary flow). A minus sign denotes a minimum value, or IS (inlet system) = FG, or $\theta = 0°$. Positive sign denotes a maximum value, or IS = RID, or $\theta = 15°$. The numbers above the signs represent the rank of significance. Greyed cells re-emphasize that the corresponding factor is the most significant (first rank). Zero means the factor has no effect.

**TABLE 4: SUMMARY OF RECOMMENDED VALUES OF ALL FACTORS.**

| Responses | IS | $Q_L$ | SR | $\Omega$ | dR | w | R2 | R3 | $\theta$ |
|---|---|---|---|---|---|---|---|---|---|
| Upstream Flow | 1 – | 0 | 0 | 2 – | 0 | 0 | 0 | 0 | 0 |

| Detachment | | | | | | | | | |
|---|---|---|---|---|---|---|---|---|---|
| Upstream Flow Dry-out | 1<br>+ | 3<br>+ | †<br>– | 2<br>– | + | + | ‡<br>+/<br>0 | – | + |
| Secondary Flow | + | + | 3<br>– | 1<br>– | 2<br>– | – | + | + | – |

†: DOE indicates that upstream flow dry-out is less likely if SR = 1.5 compared to SR = 1.2, but the difference is not significant.
‡: Plus sign is according to DOE. Comparison with an additional configuration (not a part of the initial DOE) shows that a curvier or flatter downstream wall does not affect upstream wall dry-out.

The top 3 factors are usually the flow condition factors. The only geometrical factor that makes it to the top 3 is the sump depth. This highlights the importance of inlet condition factors on the overall bearing chamber scavenge performance. Shaft speed is generally the most significant factor.

A common preferred value is minimum shaft speed. This highlights the importance to keep the shaft induced windage as low as possible to negate undesirable responses. Nevertheless, to operate the shaft at the lowest possible speed is often not practical. Alternatively, structures within the bearing chamber such as a bearing support mount can be effective in suppressing the shaft induced windage. However its impact on residence volume or residence time is unknown.

The table also highlights a possible conflict of interest. For example, in order to minimize upstream flow detachment, FG inlet system needs to be used. However, in terms of minimizing upstream flow dry-out, RID inlet system is the preferred choice. The complication is compounded by the fact that in the engine bearing chamber, the liquid flow is equivalent to a combination of FG and RID inlet systems. In this case, a designer may need to consider and weigh all factors.

Future work will incorporate the results of this study with other results from previous studies on scavenge flow in various bearing chambers and sump geometries, in various flow and operating conditions. It may prove possible to introduce a set of non-dimensionalised parameters. Additionally, a wider range of test matrices will be considered to enable generalization. This includes the properties of the working fluids, such as viscosity, surface tension, pressure and temperature. A more engine realistic scenario can be introduced by studying the effects of pressurization and venting.

## ACKNOWLEDGMENTS

The authors would like to thank Rolls-Royce plc for its financial and technical support and the UK Technology Strategy Board for its financial support of the SILOET program. We are grateful for the technical support of Aida Alvarez and Trevor Gibson of Rolls-Royce Derby on the DOE analysis. We also extend our gratitude to Dr Graham Johnson, Robert Stables, Barry Hatch, and Terry Alvey of the Gas Turbine and Transmissions Research Centre for the design and building of the test rig.

## REFERENCES

[1] Wittig, S., Glahn, A., and Himmelsbach, J., 1994, "Influence of High Rotational Speeds on Heat Transfer and Oil Film Thickness in Aero-Engine Bearing Chambers," ASME J. Eng. Gas Turbines and Power, 116, pp. 395-401.

[2] Glahn, A., and Wittig, S., 1996, "Two-Phase Air/Oil Flow in Aero Engine Bearing Chambers: Characterization of Oil Film Flows," ASME J. Eng. Gas Turbines and Power, 118, pp. 578-583.

[3] Gorse, P., Busam, S., and Dullenkopf, K., 2006, "Influence of Operating Condition and Geometry on the Oil Film Thickness in Aeroengine Bearing Chambers," ASME J. Eng. Gas Turbines and Power, 128, pp. 103-110

[4] Glahn, A., Kurreck, M., Willmann, M., and Wittig, S., 1996, "Feasibility Study on Oil Droplet Flow Investigations inside Aero Engine Bearing Chambers – PDPA Techniques in Combination with Numerical Approaches," ASME J. Eng. Gas Turbines and Power, 118, pp. 749-755.

[5] Glahn, A., Busam, S., Blair, M. F., Allard, K. L., and Wittig, S., 2002, "Droplet Generation by Disintegration of Oil Films at the Rim of a Rotating Disk," ASME J. Eng. Gas Turbines and Power, 124, pp. 117-124.

[6] Rodkey, S. C., Heister, S. D., and Collicott, S. H., 2007, "Physics of Gas Turbine Engine Bearing Chambers," 43rd AIAA/ASME/SAE/ASEE Joint Propulsion Conference and Exhibit, Cincinnati, Ohio, USA.

[7] Kurz, W., Dullenköpf, K., and Bauer, H., 2011, "The Impact of Geometry Variations on the Two-phase Flows in Aero-engine Bearing Chambers," ISABE-2011-1830, Proceedings of International Symposium on Air Breathing Engines, Gothenburg, Sweden.

[8] von Plehwe, Felic C., Krug, Matthias B., Höfler, C., and Bauer, H-J., 2016, "Experimental and Numerical Investigations on Oil Leakage Across Labyrinth Seals in Aero Engine Bearing Chambers," GT2016-56297, Proceedings of ASME Turbo Expo, Seoul, South Korea.
[9] von Plehwe, Felic C., Brox, B., Höfler, C., and Bauer, H-J., 2017, "Experimental Investigation of the Influence of Chamber Geometry on Bearing Chamber Oil Leakage," GT2017-63561, Proceedings of ASME Turbo Expo, Charlotte, North Carolina, USA.
[10] Chandra, B. W., Simmons, K., Pickering, S., and Tittel, M., 2010, "Factors Effecting Oil Removal from an Aeroengine Bearing Chamber," GT2010-22631, Proceedings of ASME Turbo Expo, Glasgow, UK.
[11] Chandra, B., Simmons, K., Pickering, S., Tittel, M., 2011 "Liquid and Gas Flow Behaviour in Highly Rotating Environment," GT2011-46430, Proceedings of ASME Turbo Expo, Vancouver, Canada.
[12] Chandra, B., Simmons, K., 2013, "Performance Comparison for Aeroengine-Type Sump Geometries," IMECE2013-62836, Proceedings of ASME International Mechanical Engineering Congress & Exposition, San Diego, California, USA.
[13] Chandra, B. W., 2006, "Flows in Turbine Engine Oil Sumps," PhD Dissertation, Purdue University.
[14] Chandra, B., Collicott, S. H., Munson, J. H., 2013, "Scavenge Flow in a Bearing Chamber with Tangential Sump Off-take," ASME J. Eng. Gas Turbines Power 135(3), 032503 (9 pages) doi:10.1115/1.4007869.
[15] Chandra, B., Collicott, S. H., Munson, J. H., 2017, "Experimental Optimization of Rolls-Royce AE3007 Sump Design," GT2017-64030, Proceedings of ASME Turbo Expo, Charlotte, North Carolina, USA.
[16] Chandra, B., Simmons, K., Pickering, S., Keeler, B., 2013, "Parametric Study into the Effect of Geometric and Operational Factors on the Performance of an Idealized Aeroengine Sump," ISABE2013-10311, Proceedings of International Symposium on Air Breathing Engines, Busan, South Korea.
[17] Chandra, B., Simmons, K., Pickering, S., Collicott, S. H., Wiedemann, N., 2013, "Study of Gas/Liquid Behaviour within an Aeroengine Bearing Chamber," ASME J. Eng. Gas Turbines Power 135(5), 051201 (11 pages) doi:10.1115/1.4007753.
[18] Antony, J., 1983, "Design of Experiments for Engineers and Scientists," Butterworth-Heinemann, New York, USA.